PCCP

Excited State Dynamics of 2'-Deoxyisoguanosine and Isoguanosine in Aqueous Solutions

Journal:	*Physical Chemistry Chemical Physics*
Manuscript ID	CP-ART-12-2021-005795.R1
Article Type:	Paper
Date Submitted by the Author:	13-Feb-2022
Complete List of Authors:	Caldero-Rodríguez, Naishka; Case Western Reserve University College of Arts and Sciences, Chemistry Crespo-Hernández, Carlos; Case Western Reserve University College of Arts and Sciences, Chemistry

ARTICLE

Excited State Dynamics of 2'-Deoxyisoguanosine and Isoguanosine in Aqueous Solutions

Received 00th January 20xx,
Accepted 00th January 20xx

DOI: 10.1039/x0xx00000x

Naishka E. Caldero-Rodríguez,[a] Carlos E. Crespo-Hernández*[a]

Photostability is thought to be an inherent property of the nucleobases required to survive the extreme ultraviolet radiation conditions of the prebiotic era. Previous studies have shown that absorption of ultraviolet radiation by the canonical nucleosides results in ultrafast internal conversion to the ground state, demonstrating that these nucleosides efficiently dissipate the excess electronic energy to the environment. In recent years, studies on the photophysical and photochemical properties of nucleobase derivatives have revealed that chemical substitution influences the electronic relaxation pathways of purine and pyrimidine nucleobases. It has been suggested that amino or carbonyl substitution at the C6 position could increase the photostability of the purine derivatives more than the substitution at the C2 position. This investigation aims to elucidate the excited state dynamics of 2'-deoxyisoguanosine (dIsoGuo) and isoguanosine (IsoGuo) in aqueous solution at pH 7.4 and 1.4, which contain an amino group at the C6 position and a carbonyl group at the C2 position of the purine chromophore. The study of these derivatives is performed using absorption and emission spectroscopies, broadband transient absorption spectroscopy, density functional, and time-dependent density functional levels of theory. It is shown that the primary relaxation mechanism of dIsoGuo and IsoGuo involves nonradiative decay pathways, where the population decays from the $S_1(\pi\pi^*)$ state through internal conversion to the ground state via two relaxation pathways with lifetimes of hundreds of femtoseconds and less than 2 ps, making these purine nucleosides photostable in aqueous solution.

Introduction

Photostability to ultraviolet radiation is likely one of the intrinsic properties necessary for RNA and DNA precursors to survive the extreme environmental conditions of prebiotic Earth.[1] Previous studies have demonstrated that the relaxation pathways of the canonical nucleosides, adenosine, guanosine, cytidine, thymidine, and uridine are primarily characterized by an ultrafast relaxation decay to the ground state, evidencing that these nucleosides efficiently dissipate the electronic energy to the environment, thus minimizing photochemical damage.[1, 2] Experimental and computational research has also demonstrated that the excited state dynamics of purine and pyrimidine derivatives are significantly influenced by the addition or removal of functional groups and the specific position at which functional groups are located.[3, 4] These modifications can affect the order and topology of the excited state potential energy surfaces that give rise to specific nuclear deformations and the accessibility to conical intersections.[3, 4]

In particular, it has been proposed that the functional group at the C2 and C6 position can significantly affect the relaxation mechanisms of the purines derivatives.[3, 5] The substitution at the C6 position has been proposed to increase the rate of internal conversion to the ground state (equated hereafter to increase in photostability) of the purine derivatives more than at the C2 position.[3, 6, 7] This statement can be supported by comparing the relaxation mechanism of the purine free base, adenine (6-aminopurine), 2-aminopurine, hypoxanthine (6-oxopurine) and 2-oxopurine in solution. The relaxation pathway of the purine free base is characterized by a slow intersystem crossing, while the population of adenine mainly decays through ultrafast internal conversion to the ground state.[3, 6] For 2-aminopurine, a competition between slow internal conversion and intersystem crossing is observed depending on the solvent.[7] An ultrafast electronic deactivation has been reported for hypoxanthine,[8] comparable to the one observed for adenine. For 2-oxopurine, recent quantum-chemical calculations predicted that intersystem crossing could compete with fluorescence emission and internal conversion to the ground state.[5]

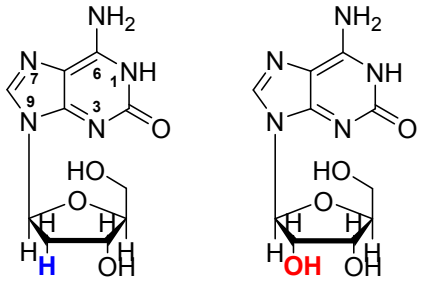

Scheme 1. Structures of 2'-deoxyisoguanosine (dIsoGuo; left) and isoguanosine (IsoGuo; right). Blue and red emphasize the difference between the systems, respectively. Standard ring numbering has been included.

[a]*Department of Chemistry, Case Western Reserve University, Cleveland, OH 44106. *Corresponding author; E-mail: carlos.crespo@case.edu;ORCID: 000-0002-3594-0890.*

†Electronic Supplementary Information (ESI) available: Steady state absorption and emission spectra of dIsoGuo and IsoGuo, DFT optimized geometries, TDDFT vertical excitation energies and Kohn-Sham orbitals for each relevant tautomer of dIsoGuo and IsoGuo, normalized kinetic decay traces for dIsoGuo and IsoGuo, transient absorption spectra of solvent-only signals, lifetimes for the solvent-only coherence signals.
See DOI: 10.1039/x0xx00000x

2'-Deoxyisoguanosine and isoguanosine contain an amino group in the C6 position and a carbonyl group in the C2 position (Scheme 1), making them constitutional isomers of the guanine nucleosides. Importantly, the isoguanine nucleobase is a product of oxidative damage to adenine in DNA/RNA and has been shown to cause mutation.[9] [10] [11] A recent study investigated the excited state dynamics of the enol N9 tautomer isoguanine in the gas phase,[12] where a barrierless photodeactivation mechanism from the $S_1(\pi\pi^*)$ state to the ground state was reported. However, to the best of our knowledge, there is no information about the electronic relaxation mechanism of the DNA/RNA isoguanine nucleosides in solution. Hence, one motivation of this study is to elucidate the excited state dynamics of 2'-deoxyisoguanosine (dIsoGuo) and isoguanosine (IsoGuo) in aqueous solution and document whether the type of sugar in the N9 position of the isoguanine chromophore affects the photophysical properties and the electronic relaxation pathways to any significant extent. It has also been reported that protonation significantly affects the photophysics and excited state dynamics of guanosine and guanosine monophosphate.[13] [14] Hence, another motivation of this study is to investigate the effect that protonation may have in the photophysics of dIsoGuo and IsoGuo in acidic conditions, where the carbonyl and amino groups in the C6 and C2 positions are interchanged compare to guanosine.

Experimental and theoretical methods

Chemicals

Isoguanosine (IsoGuo) and 2'-deoxyisoguanosine (dIsoGuo) were purchased from Berry and Associates (≥ 97% purity) and were used as received. Aqueous phosphate buffer solutions at pH 7.4 were freshly prepared, with a total concentration of 16 mM from monopotassium (KH_2PO_4) and dipotassium phosphate (K_2HPO_4) salts in ultrapure water. The pH was adjusted to pH 7.4 using sodium hydroxide (NaOH). Aqueous phosphate buffer solutions at pH 1.4, with a total concentration of 16 mM, were also freshly prepared by dissolving monosodium phosphate (NaH_2PO_4) salts and phosphoric acid (H_3PO_4) in ultrapure water. The pH was adjusted to pH 1.4 using H_3PO_4.

Steady state measurements

Steady state absorption was measured using a Cary 300 spectrophotometer. Absorption spectra were collected using a 300 nm/min scan rate, a data interval of 1.0 nm, and an average time of 0.2 seconds. Steady state emission was measured in a Cary Eclipse spectrofluorimeter. Emission spectra were obtained using a scan rate of 120 nm/min, excitation and emission slits at 5 nm, and a PMT voltage of 800 V.

Quantum chemical calculations

Quantum chemical calculations were performed using Gaussian 16 suite of programs.[15] Ground state optimizations for the *anti*- and *syn*-sugar conformations of the neutral and protonated tautomers of IsoGuo and dIsoGuo were performed using density functional theory (DFT) at the B3LYP/IEFPCM/6-311++G(d,p) level of theory in water. Time-dependent DFT (TDDFT) calculations were performed for the lowest energy tautomers at the PBE0/IEFPCM/6-311++G(d,p) level of theory in water. For ground state optimizations and vertical excitation energies (VEE), the polarizable continuum model (PCM) was used with the integral equation formalism (IEF) to model bulk solvent dielectric effects.[16] [17]

Ground state optimizations were also performed for the *anti*- and *syn*-sugar conformations of the neutral and protonated tautomers of IsoGuo and dIsoGuo with three explicit water molecules at the B3LYP/6-31+G(d,p) level of theory in water. Then, single-point energy calculations were performed for these tautomers at the B3LYP/IEFPCM/6-311++G(d,p) level of theory in water. TDDFT computations were also performed for the *anti*- and *syn*-sugar conformations of the neutral and protonated tautomers of IsoGuo and dIsoGuo with three explicit water molecules at the PBE0/IEFPCM/6-311++G(d,p) level of theory in water. Analogous TDDFT calculations were performed for the double-protonated tautomer with 2'-deoxyribose (*syn*-H1,H3,H7-dIsoGuo) in water with three explicit water molecules at the PBE0/IEFPCM/6-311++G(d,p) level of theory.

Femtosecond transient absorption spectroscopy

The excited state dynamics of dIsoGuo and IsoGuo were investigated using broadband femtosecond transient absorption spectroscopy. Laser experimental setup has been described in detail previously.[7, 18] [19] [20] Briefly, a Ti:Sapphire oscillator (Vitesse, Coherent) seeds a chirped-pulse regenerative amplifier (Libra-HE, Coherent), generating 100 fs pulses at 800 nm with a 1 kHz repetition rate. The laser output is used to pump an optical parametric amplifier (TOPAS, Quantronix/light conversion) tuned to 286 nm for transient absorption measurements. 2% of the 800 nm beam is split off and focused on a translating 2 mm CaF_2 crystal to generate the white light continuum (320 to 700 nm). Solutions in a 2 mm path length fused silica cell were continuously stirred with a Teflon stir bar throughout the experiments. A homemade software, LabView program, was used for data collection. Data analysis was performed using the Glotaran graphical user interface to the R-package TIMP software.[21]

The power of the excitation pulse at 286 nm was set to 0.5 and 0.6 mW at pH 7.4 and pH 1.4, respectively. Under these low-power conditions, the signal depends linearly on the pump power, and no hydrated electron signal from multiphoton ionization of the solvent was observed.[22] [23]In addition, under these experimental conditions, photodegradation of the samples was minimal (<1%) after completion of the laser experiments. The percentage of photodegradation was estimated from the decrease in absorbance at the absorption maximum of the lowest-energy absorption band at the end of the laser experiment relative to the absorbance of the same band for the fresh solution (i.e., before laser experiments).

Results

Steady state photophysics

Figure 1 shows the molar absorption spectra of 2'-deoxyisoguanosine (dIsoGuo) and isoguanosine (IsoGuo) in aqueous phosphate buffer solutions at pH 7.4 and pH 1.4, where the keto form of the dIsoGuo and IsoGuo predominantly exists, respectively.[24] In aqueous phosphate buffer solution at pH 7.4, dIsoGuo presents three distinctive absorption bands at 292, 247, and 206 nm, whereas IsoGuo exhibits maximum absorption at 293, 247, and 206 nm. In aqueous phosphate buffer solution at pH 1.4, dIsoGuo and IsoGuo display three absorption bands, with maxima at 284, 235, 205 nm, and 283, 235, and 206 nm, respectively. The absorption spectra are in good agreement with those reported previously in aqueous solution at pH 7 and 1 by Seela et al.[24] The pK_a values for these compounds have been reported as 3.4 and 9.8 for IsoGuo,[25] and 4.0, and 9.9 for dIsoGuo.[26] Using the Henderson-Hasselbalch relationship, dIsoGuo and IsoGuo exist as the neutral and protonated species (>99%) at pH 7.4 and 1.4, respectively, which are the focus of this work from this point forward.

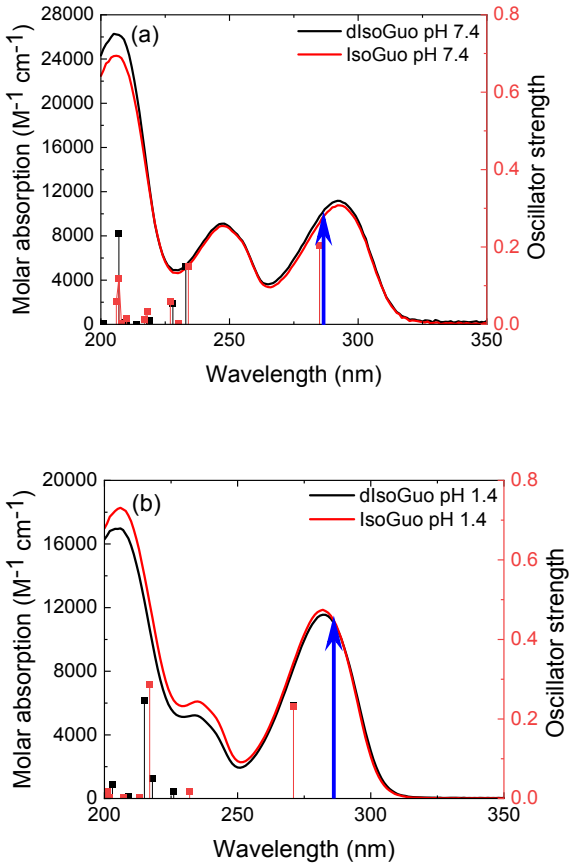

Figure 1. Molar absorption spectra of dIsoGuo (black) and IsoGuo (red) in aqueous phosphate buffer solutions at (a) pH 7.4 and (b) pH 1.4, together with the calculated vertical excitation energies (VEE, nm) and oscillator strengths for the lowest energy tautomer of each molecule, *syn*-H1-dIsoGuo and *syn*-H1-IsoGuo for the neutral species, and *syn*-H1,H3-dIsoGuo and *syn*-H1,H3-IsoGuo for the protonated species at the TD-PBE0/IEFPCM/6-311++G(d,p)//B3LYP/IEFPCM/6-311++G(d,p) level of theory in water. Blue arrows indicate the excitation wavelength used for transient absorption measurements (286 nm). Molar absorption coefficients were taken from ref.[24] at both pHs (see main text for details).

Interestingly, it was noted that the ground state absorption spectrum of the freshly prepared solution of dIsoGuo at pH 1.4 changes over time and is different from the absorption spectrum previously reported in ref. [24]. Thus, a kinetic absorption study was performed, where the absorption spectrum of the dIsoGuo at pH 1.4 was carefully measured through time. It was found that the absorption spectrum of the freshly prepared solution changes as a function of time until about 2 hours at room temperature. These spectral changes are reported in Figure 2a. A redshift with a slight decrease in absorbance in the lowest energy band, a blue shift and a decrease of the second lowest energy band around 235 nm, and a decrease in absorbance in the band around 205 nm are observed. These changes suggest that one species is converting over time to another species in the acidic solution. Hence, to further examine this idea, a fresh solution was heated for 1 minute at 64℃, and the absorption spectrum was recorded after letting the solution reach room temperature. Comparison of the absorption spectra at room temperature, before and after heating the fresh solution clearly shows a shift of the equilibrium completely towards the most stable species (Figure 2b). The heated solution was left to reach room temperature for about 10 minutes, and then the emission spectrum was obtained (Figure 2c). The same spectral behavior was observed in a second absorption study (Figure S1). Importantly, no additional absorption or emission spectral changes were observed over time after letting the heated solution reach room temperature. Therefore, the experimental results reported hereafter for dIsoGuo at pH 1.4 made use of solutions at room temperature but that were pre-heated to guarantee the investigation of the most thermodynamically stable species (see Figure 2).

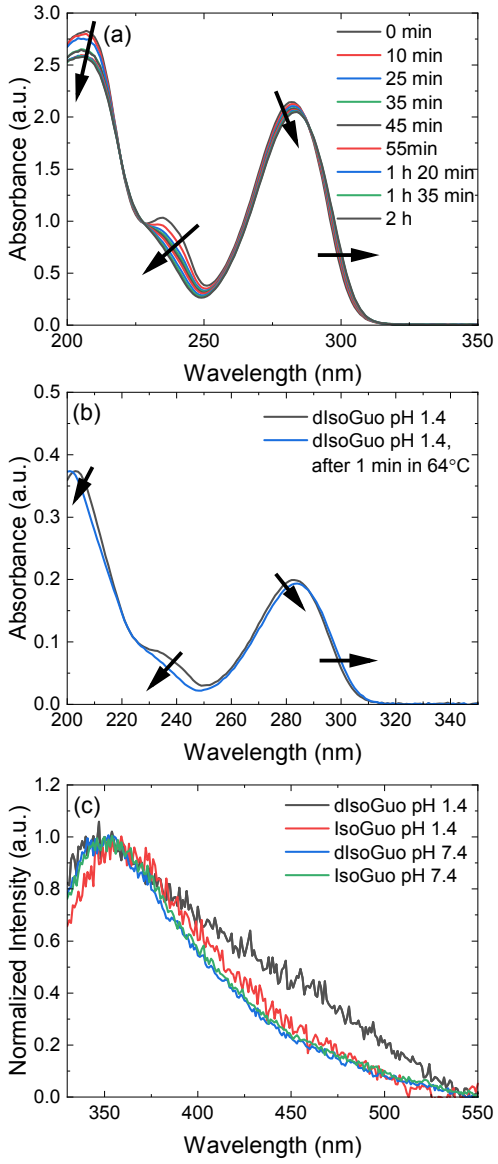

Figure 2. Ground state absorption spectra of freshly prepared dIsoGuo in aqueous phosphate buffer solution at pH 1.4 measured through time (a) at room temperature (r.t.) and (b) at room temperature before and after heating the solution at 64°C. (c) Normalized ground state emission spectra of dIsoGuo and IsoGuo at pH 1.4 (black and red, respectively) and pH 7.4 (blue and green, respectively). The emission spectrum of dIsoGuo in aqueous phosphate buffer solution at pH 1.4 in Figure 2c was recorded once the solution reached room temperature after heating the sample at 64°C. It is worth mentioning that the emission spectra of a freshly prepared solution of dIsoGuo in aqueous phosphate buffer solution at pH 1.4 and the solution after heating it at 64°C and leaving it to reach room temperature are the same. Emission spectra were obtained using an excitation wavelength of 285 nm and were recorded at 800 V, keeping both the excitation and emission slit at 5 nm, with a scan rate of 120 nm/min.

After heating the solution of dIsoGuo at pH 1.4 to 64°C and letting it cool down to room temperature, the emission spectrum shows a maximum at 345 nm with a long tail to ca. 550 nm, while the emission maximum of IsoGuo at pH 1.4 is closer to 360 nm. Conversely, the emission maximum for both dIsoGuo and IsoGuo at pH 7.4 is similar and closer to 350 nm (Figure 2c). In addition, the fluorescence spectrum of dIsoGuo at pH 1.4 exhibits an emission shoulder around 450 nm, not observed at pH 7.4 for both nucleosides, and barely observed for IsoGuo at pH 1.4. It is worth remarking that both dIsoGuo and IsoGuo can be considered nearly non-fluorescent under the experimental conditions presented, and the low emission intensity of these molecules may slightly affect the spectral shape because of the sensitivity limit of the spectrometer. It should also be remarked that we considered but did not observe any evidence of the presence of fluorescent impurities or photodegradation of the samples (see Figure S2) as the reason for the observed spectral changes reported in Figure 2.

Ground state optimizations and vertical excitation energies for the neutral and protonated species of IsoGuo and dIsoGuo in water

Ground state optimizations were performed for the *anti*- and *syn*-sugar conformations of the neutral (Scheme 2) and protonated (Scheme 3) tautomers of IsoGuo and dIsoGuo at the B3LYP/IEFPCM/6-311++G(d,p) level of theory in water (see also Tables S1 and S2). In what follows, the relative stabilization energies are defined relative to the energy of the lowest energy tautomer for each molecule optimized in the ground state (see Schemes 2 to 5). These computations were followed by TDDFT calculations for the lowest energy tautomers predicted to be available in water (*syn*-H1-dIsoGuo and *syn*-H1-IsoGuo for the neutral species, and *syn*-H1,H3-dIsoGuo and *syn*-H1,H3-IsoGuo for the protonated species) at the PBE0/IEFPCM/6-311++G(d,p) level of theory (see Tables S3, S4, S5, and S6). The vertical excitation energies (VEE) and oscillator strengths obtained for the most stable neutral and protonated tautomers of dIsoGuo and IsoGuo are also shown in Figure 1 at the TD-PBE0/IEFPCM/6-311++G(d,p)//B3LYP/IEFPCM/6-311++G(d,p) level of theory. The *syn*-sugar is the most stable conformation for the neutral and protonated species of dIsoGuo and IsoGuo. In the case of the *syn*-neutral tautomers of IsoGuo and dIsoGuo, the lowest energy tautomer contains the hydrogen at the N1 position of the purine ring (*syn*-H1 tautomer, Scheme 2), as seen for other purine nucleobases.[5, 13, 27] The relative stabilization energies for the lowest energy *anti*-conformation of the neutral tautomers of dIsoGuo and IsoGuo lie 3.47 and 3.77 kcal mol^{-1}, respectively, higher in energy than the most stable *syn*-neutral tautomer for each nucleoside. For the *syn*-protonated tautomers of IsoGuo and dIsoGuo, the lowest energy tautomers include hydrogens at the N1 and N3 positions of the purine ring (*syn*-H1,H3 tautomer, Scheme 3). The lowest energy *anti*-conformation of the protonated tautomers of IsoGuo and dIsoGuo are 5.05 and 5.18 kcal mol^{-1}, respectively, higher in energy than the most stable *syn*-protonated tautomer.

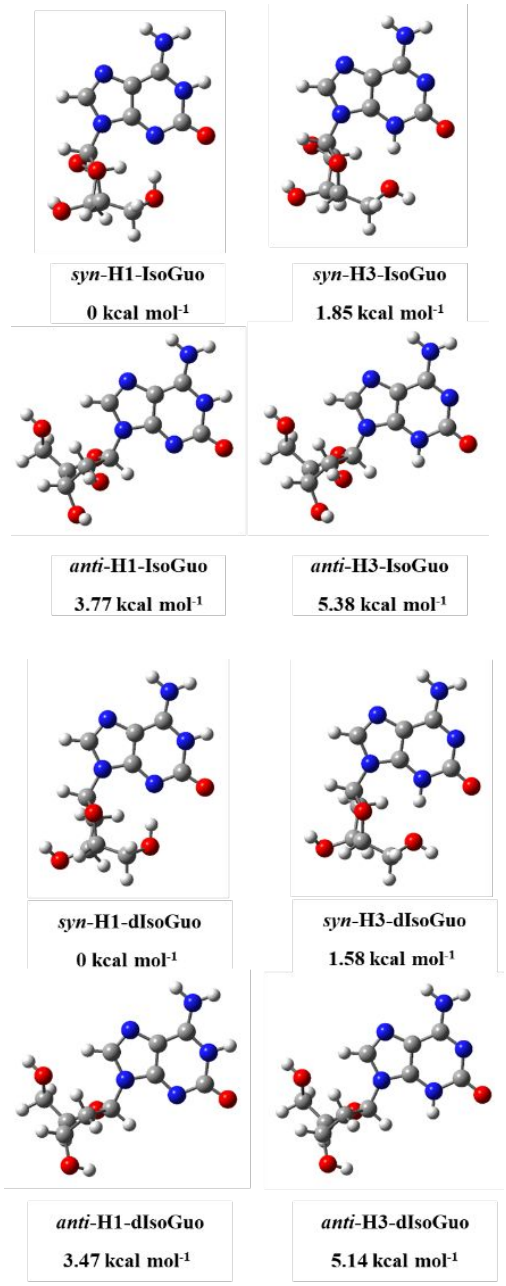

Scheme 2. Optimized structures of the *anti*- and *syn*-neutral tautomers of IsoGuo (top) and dIsoGuo (bottom) that were considered in this study with their relative stabilization energies in kcal mol^{-1}. Note that in the experiments a distribution of sugar conformations is expected to be present at room temperature in aqueous solution. Such a distribution of conformations is not expected to have a major impact on photophysical results reported in this study.

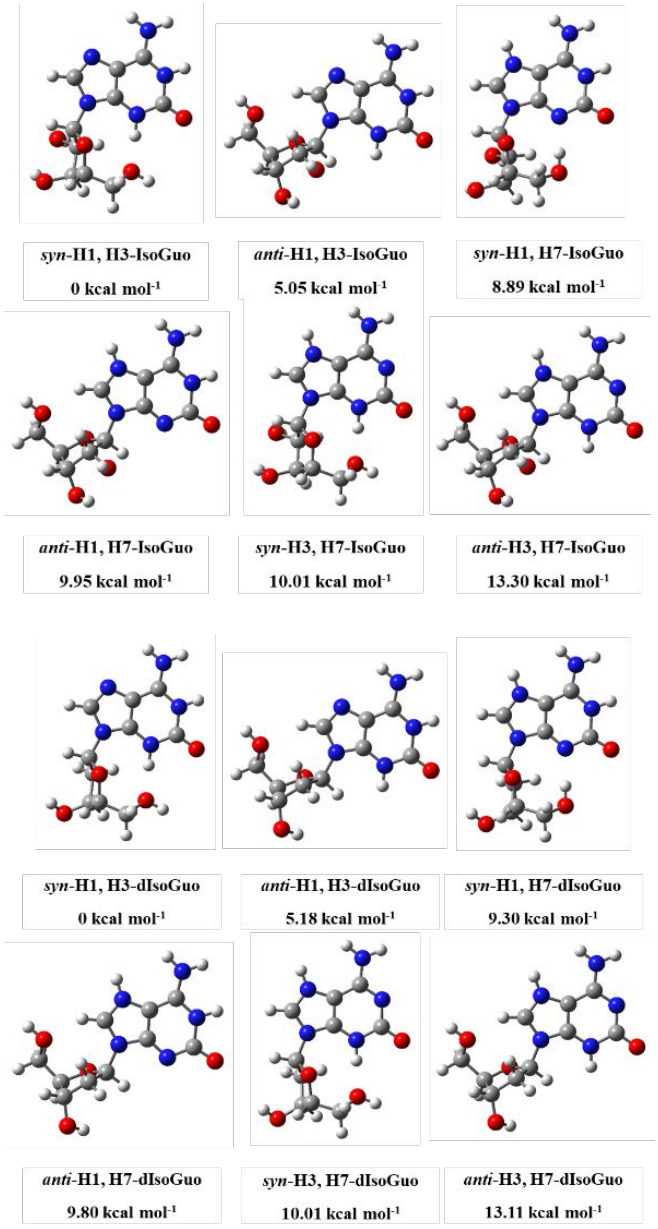

Scheme 3. Optimized structures of the *anti*- and *syn*-protonated tautomers of IsoGuo (top) and dIsoGuo (bottom) that were considered in this study with their relative stabilization energies in kcal mol^{-1}. Note that in the experiments a distribution of sugar conformations is expected to be present at room temperature in aqueous solution. Such a distribution of conformations is not expected to have a major impact on photophysical results reported in this study.

TDDFT computations predict that the S_1 state of the neutral species of IsoGuo and dIsoGuo has a ππ* character, which is labeled as ^{1}ππ*(L_a) state, using Platt's[28] notation (Tables S3 and S4). The two lowest excited triplet states exhibit ππ* character for both neutral molecules, while the T_2 state also exhibits intramolecular charge transfer (ICT) character. Similarly, the S_1 state of the lowest energy protonated species of IsoGuo and dIsoGuo is the ^{1}ππ*(L_a) state (Tables S5 and S6). The two lowest excited triplet states of the protonated IsoGuo and dIsoGuo exhibit ππ* character, with an ICT character for the second triplet excited state, as observed for the

neutral molecules. The use of ribose versus 2'-deoxyribose does not significantly affect the order and character of the excited states of the neutral and protonated tautomers at the TDDFT level of theory.

Ground state optimizations and vertical excitation energies for the neutral and protonated species of IsoGuo and dIsoGuo in water, including microsolvation with three explicit water molecules

Ground state optimizations for the *anti*- and *syn*-sugar conformations of the neutral (Scheme 4) and protonated (Scheme 5) tautomers of IsoGuo and dIsoGuo in water were also performed with microsolvation at the B3LYP/6-31+G(d,p) level of theory, followed by single-point energy calculations at the B3LYP/IEFPCM/6-311++G(d,p) level of theory (Tables S7 and S8). The computations including microsolvation confirmed that the most stable tautomer available in solution for the neutral species of dIsoGuo and IsoGuo is the *syn*-H1 tautomer. However, the relative stabilization order of the other neutral tautomers changed. Now, the *anti*-H1 tautomer is placed as the second lowest energy tautomer for both neutral dIsoGuo and IsoGuo and lies 3.30 and 2.07 kcal mol^{-1} relative to the lowest energy tautomer, respectively. In the case of the protonated species of dIsoGuo and IsoGuo, the single-point energy calculations predict that the order of the tautomers does not change when microsolvation is included. The calculations adding microsolvation predict that the lowest energy tautomer of the protonated species of IsoGuo is the *syn*-H1,H3 tautomer, followed by the *anti*-H1,H3, and the *syn*-H1,H7 tautomers, with relative energies of 4.55 and 6.46 kcal mol^{-1}, respectively. The lowest energy tautomer for the protonated species of dIsoGuo is consistent with the one obtained for IsoGuo, while the second and third lowest energy protonated tautomers of dIsoGuo now share similar stabilization energies of 6.83 kcal mol^{-1} for the *anti*-H1,H3 tautomer and 6.89 kcal mol^{-1} for the *syn*-H1,H7 tautomer.

TDDFT calculations were also performed for the lowest energy tautomer of the neutral (Tables S9 and S10) and protonated (Tables S11 and S12) IsoGuo and dIsoGuo adding microsolvation at the PBE0/IEFPCM/6-311++G(d,p)//B3LYP/6-31+G(d,p) level of theory. According to these calculations, the order and character of the excited states for both the neutral and protonated IsoGuo and dIsoGuo barely change after adding microsolvation in addition to the bulk solvation model (e.g., see Tables S6 and S12).

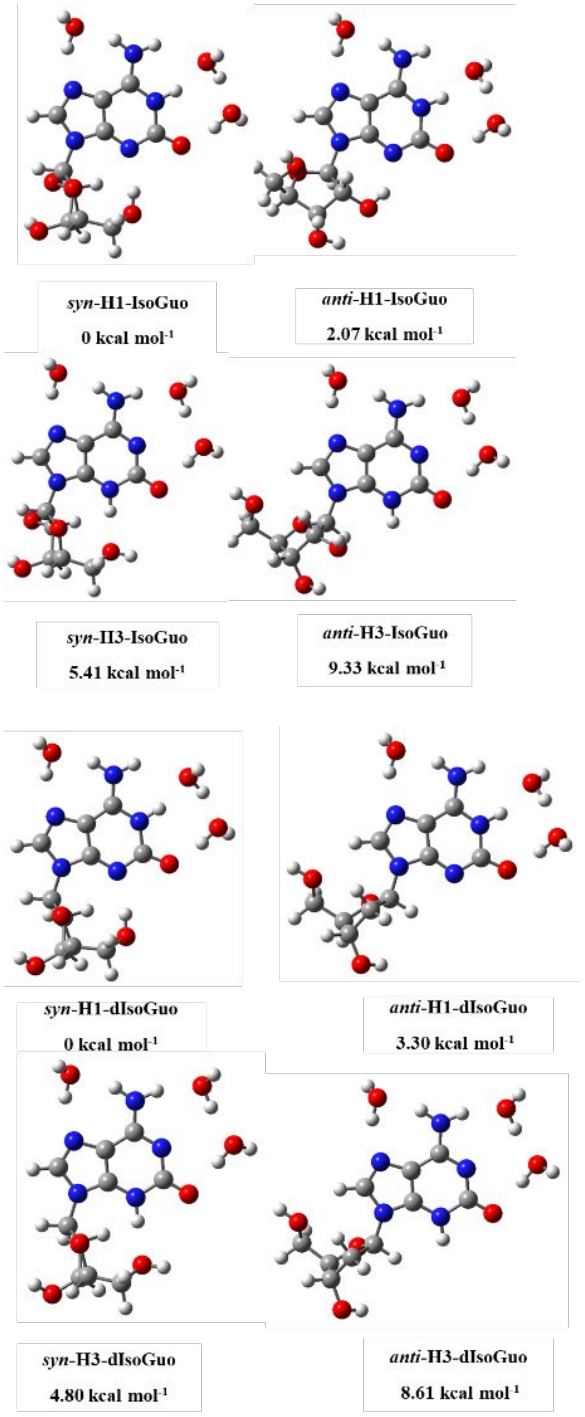

Scheme 4. Optimized structures of the *anti*- and *syn*-neutral tautomers of IsoGuo (top) and dIsoGuo (bottom) that were considered in this study with microsolvation. Relative stabilization energies were included in kcal mol^{-1}. Note that in the experiments a distribution of sugar conformations and water-nucleoside hydrogen bonding patterns are expected to be present at room temperature in aqueous solution, which are not expected to have a major impact on photophysical results reported in this study.

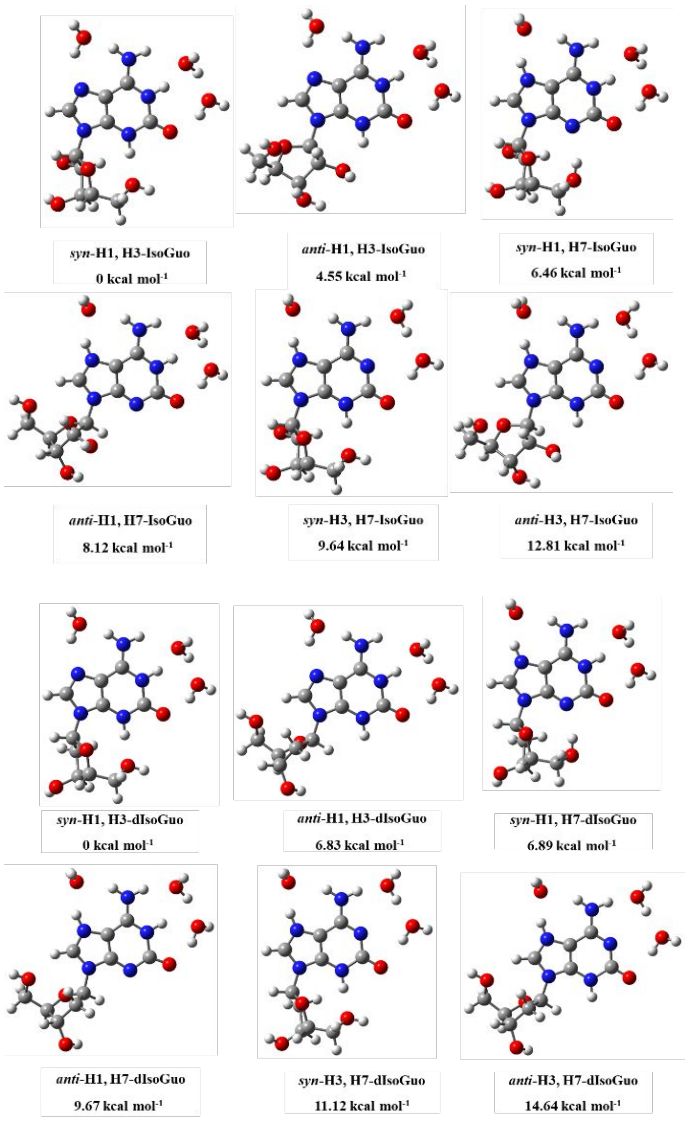

Scheme 5. Optimized structures of the *anti*- and *syn*-protonated tautomers of IsoGuo (top) and dIsoGuo (bottom) that were considered in this study with microsolvation. Relative stabilization energies were included in kcal mol^{-1}. Note that in the experiments a distribution of sugar conformations and water-nucleoside hydrogen bonding patterns are expected to be present at room temperature in aqueous solution, which are not expected to have a major impact on photophysical results reported in this study.

VEE and oscillator strengths were also obtained for the protonated tautomers *anti*-H1,H3-dIsoGuo, *syn*-H3,H7-dIsoGuo, and double-protonated tautomer *syn*-H1,H3,H7-dIsoGuo with microsolvation at the same level of theory (Tables S13, S14, and S15) for comparison purposes (the reason will be explained below). The first singlet excited state of *anti*-H1,H3-dIsoGuo, *syn*-H3,H7-dIsoGuo and *syn*-H1,H3,H7-dIsoGuo have a ππ* character, with T_1 and T_2 states with ππ* and ππ*(ICT) characters, respectively. For *syn*-H3,H7-dIsoGuo and *syn*-H1,H3,H7-dIsoGuo, the stabilization of the third triplet excited state is observed, exhibiting a ππ*(ICT) character.

Femtosecond transient absorption spectroscopy

Figure 3 presents the transient absorption spectroscopy measurements for dIsoGuo and IsoGuo at pH 7.4. The population of three transient absorption bands with a maximum around 575 and 450 nm and at shorter wavelengths at ca. 330 nm is observed within the cross correlation of the pump and probe beams (Figures 3a and d). After reaching time zero, there is an increase in intensity around 350 nm, together with a small decrease in amplitude in the band around 450 and 625 nm (Figures 3b and e). The decay of the transient absorption bands occurs after ca. 0.50 ps for both dIsoGuo and IsoGuo (Figures 3c and f), but the wavelengths between ca. 450 to 700 nm seem to decay faster than those between ca. 320 to 450 nm (Figure S3).

Global and target analyses of the transient absorption data were performed using a two-component sequential kinetic model (Figure 4a). Lifetimes of (0.30 ± 0.01) ps and (0.95 ± 0.02) ps were extracted from this analysis. The same analysis was performed for IsoGuo, and a similar behavior is observed (Figure 4c), where lifetimes of (0.24 ± 0.02) ps and (1.33 ± 0.02) ps were obtained. The second lifetime for IsoGuo is slightly longer than the one observed for dIsoGuo, which agrees with the fact that IsoGuo takes an additional 3.62 ps to decay to the ground state (Figure 3f). The evolution associated difference spectra (EADS) extracted from the global and target analyses of the transient absorption data are shown in Figure 4b for dIsoGuo and Figure 4d for IsoGuo, respectively. It should be remarked that the solvent signal may have a small contribution to the initial dynamics (< 0.3 ps) at probe wavelengths below ca. 500 nm. This is suggested by an additional analysis performed fitting the transient absorption data of the solvent-only signal with a one-component exponential kinetic model (Figure S4, Table S16).

Previously, it has been observed that the rate of vibrational cooling in the ground state of the DNA and RNA monomers varies strongly with probe wavelength, where short probe wavelengths present long lifetimes.[29 30 31 32] However, analysis of the data shown in Figure 3 did not provide evidence to support that the longer decay signal varies with probe wavelength in neither dIsoGuo nor IsoGuo, which seems to rule out the possibility of vibrational cooling in the ground state.

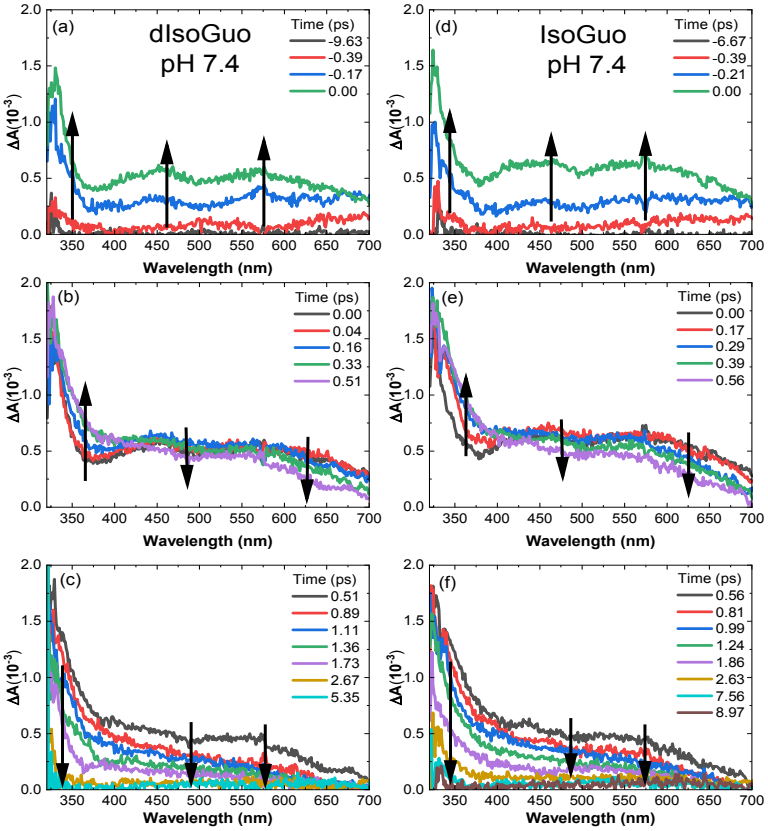

Figure 3. The transient absorption spectra of dIsoGuo (a-c) and IsoGuo (d-f) in aqueous phosphate buffer solution at pH 7.4, following 286 nm excitation. Time zero was determined at the maximum amplitude of absorption, within the cross correlation of the pump and probe beams, in panels (a) and (d) of dIsoGuo and IsoGuo, respectively.

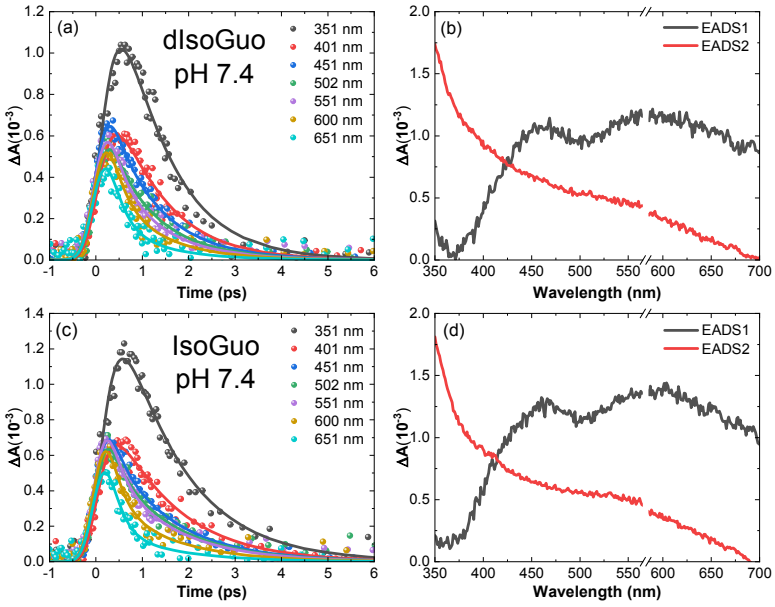

Figure 4. Representative kinetic decay traces of (a) dIsoGuo and (c) IsoGuo in aqueous phosphate buffer solution at pH 7.4, featuring analysis using a two-component sequential kinetic model. Evolution associated difference spectra (EADS) of (b) dIsoGuo and (d) IsoGuo corresponding to the 350 to 700 nm region. Notice that there is a break in the abscissa of Figures b and d to conceal the overtone of the pump beam.

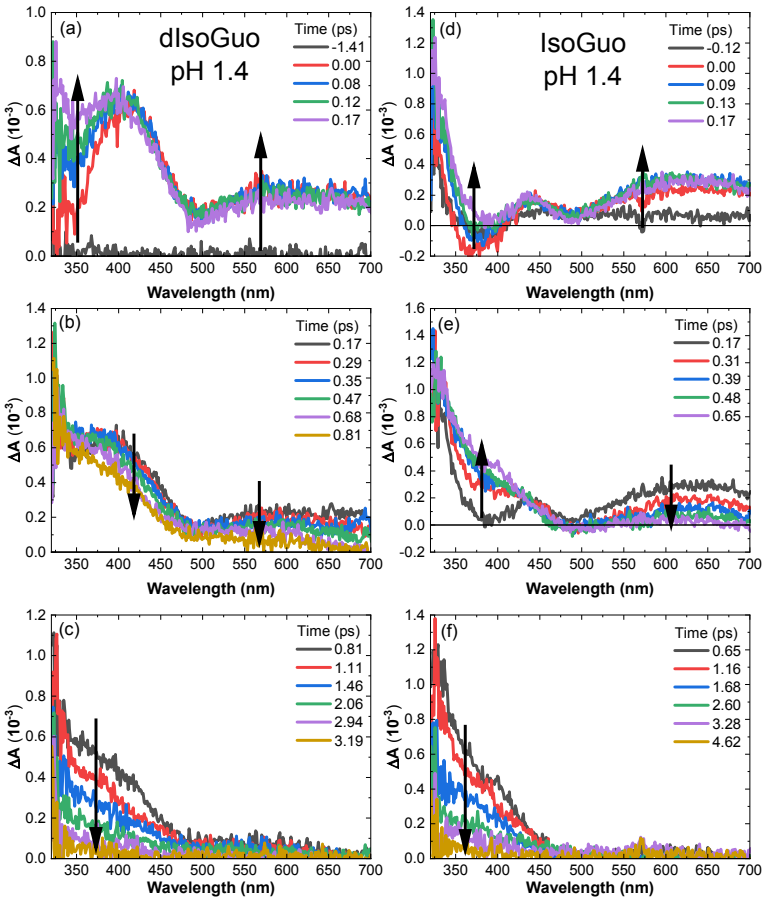

Figure 5. The transient absorption spectra of dIsoGuo (a-c) and IsoGuo (d-f) in aqueous phosphate buffer solution at pH 1.4, following 286 nm excitation. Time zero was determined at the maximum amplitude of the stimulated emission band of dIsoGuo and IsoGuo at 345 and 365 nm, respectively.

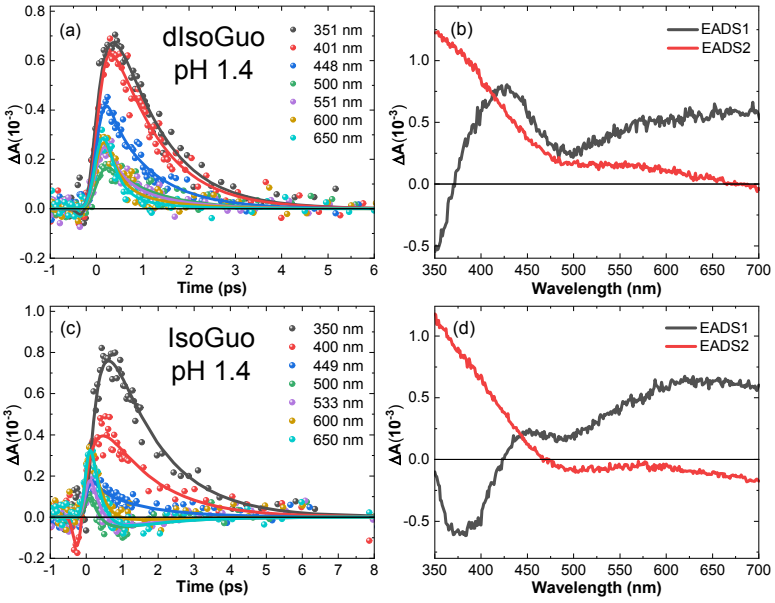

Figure 6. Representative kinetic decay traces of (a) dIsoGuo and (c) IsoGuo in aqueous phosphate buffer solution at pH 1.4, featuring analysis using a two-component sequential kinetic model. Evolution associated difference spectra (EADS) of (b) dIsoGuo and (d) IsoGuo corresponding to the 350 to 700 nm region.

The transient absorption spectroscopy measurements for dIsoGuo at pH 1.4 are presented in Figures 5a, b, and c. The formation of two transient absorption bands with a maximum around 600 and 410 nm was observed within the cross correlation of the pump and probe beams. Stimulated emission is observed around 345 nm, overshadowed by transient species absorbing in that

spectral region (Figure 5a). The latter feature agrees with the maximum of the steady state emission of dIsoGuo (Figure 2c). After reaching time zero, there is an increase in intensity, mainly around 345 nm, while the band around 600 nm remains constant (Figure 5a). Subsequently, a decrease in amplitude is observed in the region at ca. 450 nm, with the simultaneous decay of the visible band within 0.8 ps (Figure 5b). The decay of the UV band is observed up to ca. 3 ps (Figure 5c), showing that the probe wavelengths between ca. 475 to 700 nm decay at a different rate than those between ca. 320 to 475 nm (see Figure S5). Global and target analyses of the transient absorption data were performed using a two-component sequential kinetic model (Figure 6a), yielding lifetimes of (0.25 ± 0.01) ps and (0.99 ± 0.02) ps.

Figures 5d, e, and f present the transient absorption spectroscopy measurements for IsoGuo in aqueous phosphate buffer solution at pH 1.4. The formation of transient absorption bands with a maximum around 600 and 445 nm is observed within the cross correlation of the pump and probe beams. Stimulated emission is observed around 365 nm, which agrees with the steady state emission spectrum (Figure 2c). There is an increase in intensity at shorter probe wavelengths than ca. 390 nm after reaching time zero, while no significant changes are observed in the absorption bands around 445 and 600 nm (Figure 5d). Then, the intensity at shorter probe wavelengths than ca. 425 nm continues to increase concurrently with the decay of the band around 600 nm within 0.6 ps (Figure 5e). During the last 4 ps, the decay of the residual band at shorter wavelengths than ca. 450 nm occurs for IsoGuo (Figure 5f and Figure S5). Transient absorption data were fitted using a two-component sequential kinetic model (Figure 6c), yielding lifetimes of (0.29 ± 0.01) ps and (1.40 ± 0.04) ps. As noted above for solutions at pH 7.4, it is worth noting that the analysis performed for both dIsoGuo and IsoGuo at pH 1.4 did not provide evidence to support that the longer decay signal is probe wavelength dependent, which seems to rule out the possibility of vibrational cooling in the ground state.[29 30 31 32] In addition, it should be remarked that the solvent signal may have a small contribution to the initial dynamics (< 0.25 ps) at probe wavelengths below ca. 400 nm, as evidenced by additional analysis performed for the transient absorption data of the solvent-only signal (Figure S6, Table S16). The evolution associated difference spectra extracted from the global and target analyses of the transient absorption data at pH 1.4 are shown in Figure 6b for dIsoGuo and Figure 6d for IsoGuo.

Discussion

Quantum chemical calculations and steady state measurements

The *syn*-H1-form is the most stable neutral tautomer available in solution at pH 7.4 for both dIsoGuo and IsoGuo, according to DFT calculations at the B3LYP/IEFPCM/6-311++G(d,p) level of theory (Tables S1 and S2). These calculations are in agreement with previous studies showing that the most stable tautomer for isoguanine contains a hydrogen in the N1 position in aqueous solution,[33] as it has been observed for other purine nucleobases.[5, 27 13] In addition, the VEE and oscillator strengths calculated for the neutral *syn*-H1 tautomers of both nucleosides agree with the experimental absorption spectra shown in Figure 1a, further supporting the prediction from calculations. Interestingly, previous calculations for isoguanine and 9-methylisoguanine have predicted that the tautomer with the hydrogen in the N3 position is also available in aqueous solution.[33] According to the calculations reported in this study for the nucleosides, the *syn*-H3 tautomers are the second lowest energy tautomers but are not predicted to be available in aqueous solution at room temperature.

The *syn*-H1,H3 form is predicted to be the most stable protonated tautomer available in solution for IsoGuo at pH 1.4, in agreement with the results by Rogstad et al. for the protonated isoguanine and 9-methylisoguanine.[33, 34] In general, the assignments for the lowest neutral and protonated tautomers of dIsoGuo and IsoGuo were further confirmed by performing DFT computations at the B3LYP/6-31+G(d,p) level of theory by adding microsolvation to take into consideration explicit hydrogen bonding interactions (Tables S7 and S8). VEE and oscillator strengths agree with the steady state absorption data, except for the case of dIsoGuo in solution at pH 1.4, where the VEE and oscillator strengths disagree with the final absorption spectrum of dIsoGuo recorded after waiting 2 hours of equilibration at room temperature (recall Figure 2) or after heating the fresh solution for 1 minute at 64°C (Figure S7). The reason for this exception is explained next.

The steady state absorption spectra of dIsoGuo in aqueous phosphate buffer solution at pH 1.4 presented in Figure 2a and b reveals spectral changes occurring over time and as a function of temperature. These spectral changes are thought to be due to a relatively slow protonation of the single protonated tautomer of dIsoGuo converting over time to the double-protonated species. This idea is supported by measurements of the absorption spectra collected before and after increasing the temperature of the freshly prepared solution to 64 °C, showing that the absorption spectrum of the pre-heated solution after reaching room temperature is equal to the one of the freshly prepared solution after waiting for equilibration for two hours at room temperature (Figures 2a and b, Figure S1). VEE and oscillator strengths of the calculated lowest energy protonated tautomer, *syn*-H1,H3-dIsoGuo (Table S12), are in good agreement only with the absorption spectrum of the freshly prepared solution of dIsoGuo at pH 1.4 (Figure S8). VEE and oscillator strengths were also calculated for the double-protonated dIsoGuo (*syn*-H1,H3,H7-dIsoGuo) with microsolvation to perform a comparison with the experimental absorption spectrum of dIsoGuo at pH 1.4 after 2 hours of equilibration at room temperature or after heating the fresh solution for 1 minute at 64°C (Table S15). The S_1 ($\pi\pi^*$) state of the *syn*-H1,H3,H7-dIsoGuo has an energy of 4.6 eV and a significant oscillator strength of 0.2690. VEE and oscillator strengths of the *syn*-H1,H3,H7-dIsoGuo best support the experimental absorption spectrum of dIsoGuo in aqueous phosphate buffer solution at pH 1.4 after 2 hours at room temperature or after heating the fresh solution for 1 minute at 64°C (Figure S8). With this

information, it can be proposed that an equilibrium in dIsoGuo in aqueous phosphate buffer solution at pH 1.4 shifts from *syn*-H1,H3- to the *syn*-H1,H3,H7-dIsoGuo at room temperature over time. This implies that the *syn*-H1,H3,H7-dIsoGuo is the most stable tautomer available in solution for dIsoGuo at pH 1.4. We remark that the second lowest energy tautomer of the protonated dIsoGuo, *anti*-H1,H3-dIsoGuo (Table S13), was also considered, however, this tautomer is not predicted to be available in solution, with a relative energy of 6.83 kcal mol^{-1} at the level of theory used in this study (Table S8).

The results from the steady state and calculations presented in this study for dIsoGuo at pH 1.4 are further supported by previous NMR and DFT measurements for protonated isoguanine in DMSO-d_6 performed by Dybiec and Gryff-Keller.[35] Their experimental results could only be reproduced by considering an equilibrium between species, where 73.5 % was attributed to the protonated H3,H7 of isoguanine, in our case, *syn*-H3,H7-dIsoGuo, and 26.5% to a double-protonated species of isoguanine.[35] However, our calculations predict that *syn*-H3,H7-dIsoGuo has a relative energy of 11.12 kcal mol^{-1} higher than *anti*-H1,H3-dIsoGuo, supporting the idea that the double-protonated species are the ones present in solution (Table S8). Indeed, Goddard and coworkers have shown that the microscopic pK_a values for the N1, N3, and N7 positions of the isoguanine are 4.0, 3.8, and between 1.1 – 1.8,[33] respectively, which makes the double protonation possible under the acidic conditions used in our study.

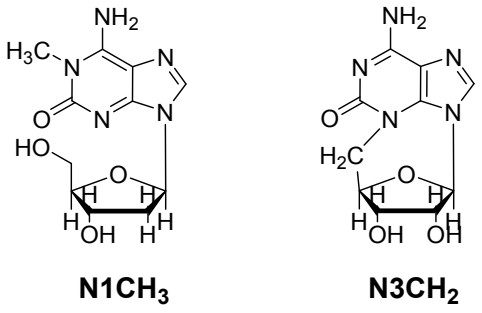

Scheme 6. Structures of the H1 fixed tautomer ($N1CH_3$) and H3 fixed tautomer ($N3CH_2$) presented in ref. [24].

In addition, the absorption spectra of the 2'-deoxy-1-methylisoguanosine (6-amino-9-((2*R*,4*S*,5*R*)-4-hydroxy-5-(hydroxymethyl)tetrahydrofuran-2-yl)-1-methyl-1,9-dihydro-2*H*-purin-2-one) and the N3-isoguanine nucleoside derivative ((8*R*,9*S*,10*R*,11*R*)-3-amino-9,10-dihydroxy-8,9,10,11-tetrahydro-5*H*,7*H*-8,11-epoxy[1,3]diazocino[1,2,3-*cd*]purin-5-one) in water at pH 7 and pH 1 (Scheme 6), taken from ref. [24] were also digitalized to compare them with the absorption spectra of dIsoGuo and IsoGuo at each respective pH. The steady state absorption spectra of these two derivatives at pH 1 and pH 7 can be used to make a qualitative comparison with the absorption spectra of dIsoGuo and IsoGuo under the same experimental conditions to further support which species are available in solution. This comparison can be justified because methylation at the N1 position in 2'-deoxy-1-methylisoguanosine or the formation of a methylene bridge between the purine and the ribose in N3-isoguanine nucleoside derivative blocks tautomerization in these derivatives (Scheme 6), but the absorption spectrum of the primary isoguanine chromophore remains practically unperturbed. The minor role of methylation on the absorption spectra of other purine free base derivatives is documented in the literature. [2 3] The 2'-deoxy-1-methylisoguanosine represents the H1 fixed tautomer ($N1CH_3$) by adding the methyl group at the N1 position, and the N3-isoguanine nucleoside derivative represents the H3 fixed tautomer ($N3CH_2$) by containing a CH_2 group at the N3 position. The comparison of the absorption spectra at ca. pH 7 (Figure S9a) shows similarities between IsoGuo and dIsoGuo with the $N1CH_3$, supporting the idea that the *syn*-H_1 form is the primary tautomer available in solution at pH 7.4, in agreement with our calculations. At pH 1, it is also observed that the absorption spectrum of IsoGuo agrees with the absorption spectrum of the $N1CH_3$ derivative. On the one hand, the absorption spectra of the $N1CH_3$ derivative at pH 7 and pH 1, used by Seela and coworkers, also agree with the absorption spectra for the lowest energy tautomer for the neutral form of dIsoGuo and IsoGuo (*syn*-H_1 form) and with the absorption spectrum for the protonated IsoGuo (*syn*-H1,H3 form), respectively (Figures S9a and b). On the other hand, the absorption spectrum of the protonated form of dIsoGuo after 1 min in 64°C agrees with the absorption spectrum of the $N3CH_2$ derivative at pH 1 (Figure S9b), supporting that a different protonated species than that for the protonated IsoGuo contribute to the absorption spectrum for the protonated dIsoGuo. Hence, this comparison further supports that the species in solution for the protonated dIsoGuo convert over time to the double-protonated species at room temperature in dIsoGuo in aqueous phosphate buffer solution at pH 1.4.

Excited state dynamics at pH 7.4

According to the experimental and computational results, it can be proposed that the primary relaxation mechanism for the *syn*-H1 form of dIsoGuo and IsoGuo in aqueous phosphate buffer solution at pH 7.4 involves a nonradiative relaxation from the initially populated $S_1(\pi\pi^*)$ state to the ground state. Specifically, it is proposed that excitation at 286 nm results in an ultrafast branching of the population, following the C2 and C6 reaction coordinates, as observed for guanine and other purine derivatives in solution.[3, 36 37 38] The population in the $S_1(\pi\pi^*)$ state travels through the potential energy surface to reach a conical intersection ((S_1/S_0) CI_1) with the ground state with a lifetime of τ_1 = (0.30 ± 0.01) ps for dIsoGuo and τ_1 = (0.24 ± 0.02) ps for IsoGuo. Lifetimes of τ_2 = (0.95 ± 0.02) ps for dIsoGuo and τ_2 = (1.33 ± 0.02) ps for IsoGuo are proposed to correspond to internal conversion to the ground state, suggesting the presence of an energy barrier to access a second (S_1/S_0) CI_2 conical intersection. The EADS were extracted from the analysis of the broadband data reported in Figures 3a, b, and c for dIsoGuo and from the data reported in Figures 3d, e, and f for IsoGuo, using a two-component kinetic model (Figure 4). The black EADS is associated with the excited state absorption of the $S_1(\pi\pi^*)$ state (Figures 3a and d). The red EADS can tentatively be assigned to the absorption

spectrum of the $S_1(\pi\pi^*)$ state near the (S_1/S_0) CI_2 (Figures 3c and f). Scheme 7 depicts the proposed relaxation mechanism based on the experimental and computational data currently available to us. However, it is important to remark that high-level calculations are needed to fully map the excited state potential energy surfaces and proposed CIs of dIsoGuo and IsoGuo.

The results presented above suggest that the interchange of the carbonyl and the amino functional groups at the C2 and C6 positions of the purine chromophore can modulate the photophysical properties and electronic relaxation pathways of the purine derivatives. For example, focusing on the 2'-deoxyriboside nucleosides, 2'-deoxyguanosine (dG) exhibits an absorption spectrum with a maximum at 253 nm for the lowest energy band and a maximum at 334 nm for the emission spectrum in water.[39] In contrast, the lowest energy band of the absorption spectrum of dIsoGuo is redshifted by ca. 39 nm to 292 nm, whereas the emission spectrum is also redshifted by ca. 16 nm to 350 nm in aqueous phosphate buffer solution at pH 7.4. Similarly, recent studies present time-resolved data that suggest that the excited state dynamics of dG after 285 nm excitation involve the population of $^1\pi\pi^*$ and $^1\pi\sigma^*$ states in neutral aqueous solutions,[39 40 41 42] which internally convert to the ground state in 0.8 ps, and 2.0 ps, respectively.[39] In contrast, the population of a $^1\pi\sigma^*$ state is not observed in this study in the excited state dynamics of dIsoGuo in aqueous phosphate buffer solution at 7.4. Photophysical and excited state dynamics differences are also observed between IsoGuo and guanosine[13 14 23 30 37 43] in neutral aqueous solutions.

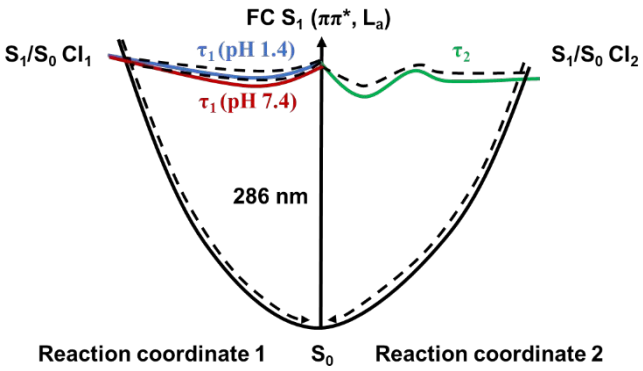

Scheme 7. Proposed excited state relaxation for dIsoGuo and IsoGuo according to the experimental and computational results. High-level calculations are needed to better understand the excited state dynamics of dIsoGuo and IsoGuo in aqueous solution.

Excited state dynamics at pH 1.4

The primary electronic process for *syn*-H1,H3,H7-dIsoGuo and *syn*-H1,H3-IsoGuo upon excitation at 286 nm involves the population of the $S_1(\pi\pi^*)$ state in aqueous phosphate buffer solution at pH 1.4. As described for solutions at pH 7.4, an ultrafast branching of the population through the C2 and C6 reaction coordinates is proposed for dIsoGuo and IsoGuo in aqueous phosphate buffer solution at pH 1.4. We argue that τ_1 = (0.25 ± 0.01) ps and τ_1 = (0.29 ± 0.02) ps correspond to a fraction of the population in the $S_1(\pi\pi^*)$ state decaying through internal conversion to the ground state through (S_1/S_0) CI_1 for dIsoGuo and IsoGuo, respectively. It is proposed that a smaller energy barrier needs to be overcome when the population travels from the $S_1(\pi\pi^*)$ minimum to the (S_1/S_0) CI_1 at pH 1.4, corresponding to the faster decay of the visible band observed in Figures 5b and e. τ_2 = (0.99 ± 0.02) ps for dIsoGuo and τ_2 = (1.40 ± 0.04) ps for IsoGuo are proposed to correspond to the movement of another fraction of the population away from the Franck-Condon (FC) region towards a second conical intersection that then internally converts to the ground state. An energy barrier needs to be overcome to access this (S_1/S_0) CI_2 as proposed for the neutral species. The black EADS (Figure 6b) extracted from the global analysis is proposed to correspond to the excited state absorption of the $S_1(\pi\pi^*)$ state observed in Figure 5a. The red EADS is tentatively assigned to the absorption spectrum of the $S_1(\pi\pi^*)$ state near the (S_1/S_0) CI_2 (Figure 6b). The same analysis was performed for the broadband data of IsoGuo in aqueous phosphate buffer solution at pH 1.4 (Figures 5d, e, and f), and a similar behavior compared to dIsoGuo can be observed in the EADS (Figure 6d). Scheme 7 presents the proposed relaxation mechanism based on the experimental and computational data currently available to us. However, we stress that multiconfigurational calculations are needed to better understand the topologies of the excited state potential energy surfaces and to locate the putative CIs in protonated dIsoGuo and IsoGuo.

Interestingly, despite the observation that IsoGuo and dIsoGuo are present as the protonated and double-protonated forms in the aqueous phosphate buffer solution at pH 1.4, there are no significant differences between the excited state dynamics of both transient species, *syn*-H1,H3-IsoGuo, and *syn*-H1,H3,H7-dIsoGuo, which decay with very similar rates. Contrary to what is observed in Guo and GMP,[13 30] the dynamics of dIsoGuo and IsoGuo are not significantly affected by a change in pH from 1.4 to 7.4. The neutral and single- and double-protonated species of dIsoGuo and IsoGuo exhibit similar excited state dynamics, and the presence of a deoxy- or ribo-sugar does not significantly affect the dynamics (Scheme 7). Protonation of Guo[30] and GMP[13] leads to the observation of hundreds of picoseconds long-lived fluorescence decay signal in aqueous solution at pH 2, which is not observed in our study for IsoGuo and dIsoGuo at pH 1.4. Of note, the transient absorption data of IsoGuo at pH 1.4 shows a negative change in amplitude around 485 nm (Figure 5e), which may be associated with a second $^1\pi\pi^*$minimum, analogous to the second minimum, $L_{a\,min}$, proposed by Kovalenko and coworkers.[13] However, multiconfigurational calculations are needed to reveal the topology of the excited state potential energy surfaces.

Another difference between guanine and isoguanine monomers is the observation by Cheng et al.[39] and Krul et al.[23] that the excited state dynamics of dG, 2'-deoxyguanosine 5'-monophosphate (dGMP), and GMP in water and methanol provided evidence for two main nonradiative relaxation pathways involving the decay of the lowest excited $^1\pi\pi^*(L_a)$ state and a weakly emissive state assigned to a $^1\pi\sigma^*$ state. In contrast, our experimental (Figure S10) and

computational results do not seem to support the involvement of a $^1\pi\sigma^*$ state in the excited state dynamics of dIsoGuo and IsoGuo. Collectively, the interchange of the carbonyl and amino groups in the C6 and C2 positions have a major effect on the photophysical properties, the topology of the excited state potential energy surfaces, and excited state dynamics of these molecules.

Conclusion

The steady state properties and the excited state dynamics of dIsoGuo and IsoGuo in aqueous phosphate buffer solutions at pH 7.4 and pH 1.4 were investigated in this study, complemented with calculations at the DFT and TDDFT levels of theory. Upon excitation at 286 nm, an ultrafast branching of the population is proposed, where the population follows different reaction coordinates to access a conical intersection and nonradiatively decay back to the ground state (Scheme 7). At pH 7.4, *syn*-H1 forms of dIsoGuo and IsoGuo populate the $S_1(\pi\pi^*)$ state, from where the population traverses to reach the (S_1/S_0) CI_1 and internally convert to the ground state in 0.30 ps and 0.24 ps, respectively, while an energy barrier needs to be overcome to access the (S_1/S_0) CI_2 with lifetimes of 0.95 ps for *syn*-H1-dIsoGuo and 1.33 ps for *syn*-H1-IsoGuo. At pH 1.4, a similar relaxation mechanism is proposed for *syn*-H1,H3,H7-dIsoGuo and *syn*-H1,H3-IsoGuo with a τ_1 of 0.25 ps and 0.29 ps, and a τ_2 of 0.99 ps and 1.40 ps.

Collectively, the interchange of the carbonyl and amino groups at the C6 and C2 positions has a major impact on the photophysical properties, the topology of the excited state potential energy surfaces, and excited state dynamics of the isoguanine versus guanine monomers. It is shown that dIsoGuo and IsoGuo are not significantly affected by the change in pH, where the neutral and single- and double-protonated species of dIsoGuo and IsoGuo exhibit similar excited state dynamics, and the presence of a deoxy- or ribo-sugar does not significantly affect the dynamics. High-level multiconfigurational calculations are needed to fully map the excited state potential energy surfaces and proposed CIs of dIsoGuo and IsoGuo.

Author contributions

Naishka E. Caldero-Rodríguez: investigation, formal analysis, writing-original draft, writing-review and editing
Carlos E. Crespo-Hernández: conceptualization, funding acquisition, project administration, resources, supervision, visualization, validation, writing-review and editing

Conflicts of interest

There are no conflicts to declare.

Acknowledgments

The authors acknowledge funding from the National Science Foundation (Grant No. CHE-1800052). This work made use of the High-Performance Computing Resource in the Core Facility for Advanced Research Computing at Case Western Reserve University.

References

1. A. A. Beckstead, Y. Zhang, M. de Vries and B. Kohler, *Phys. Chem. Chem. Phys.*, 2016, **18**.
2. C. E. Crespo-Hernández, B. Cohen, P. M. Hare and B. Kohler, *Chem. Rev.*, 2004, **104**, 1977-2019.
3. C. E. Crespo-Hernández, L. Martínez-Fernández, C. Rauer, C. Reichardt, S. Mai, M. Pollum, P. Marquetand, L. González and I. Corral, *J. Am. Chem. Soc.*, 2015, **137**, 4368-4381.
4. M. Barbatti and H. Lischka, *J. Phys. Chem. A.*, 2007, **111**, 2852-2858.
5. L. Martínez-Fernández, S. Arslancan, D. Ivashchenko, C. E. Crespo-Hernández and I. Corral, *Phys. Chem. Chem. Phys.*, 2019, **21**, 13467-13473.
6. B. Cohen, P. M. Hare and B. Kohler, *J. Am. Chem. Soc.*, 2003, **125**, 13594-13601.
7. C. Reichardt, C. Wen, R. A. Vogt and C. E. Crespo-Hernández, *Photochem. Photobiol. Sci.*, 2013, **12**, 1341-1350.
8. J. P. Villabona-Monsalve, R. Noria, S. Matsika and J. Peón, *J. Am. Chem. Soc.*, 2012, **134**, 7820-7829.
9. H. Kamiya and H. Kasai, *FEBS Lett.*, 1996, **391**, 113-116.
10. J. Tchou and A. P. Grollman, *Mutation Research*, 1993, **299**, 277-287.
11. H. Kamiya and H. Kasai, *Biochemistry*, 1997, **36**, 11125–11130.
12. G. Gate, R. Szabla, M. R. Haggmark, J. Šponer, A. L. Sobolewski and M. S. de Vries, *Phys. Chem. Chem. Phys.*, 2019, **21**, 13474-13485.
13. V. Karunakaran, K. Kleinermanns, R. Improta and S. A. Kovalenko, *J. Am. Chem. Soc.*, 2009, **131**, 5839-5850.
14. J. Peon and A. H. Zewail, *Chem. Phys. Lett.*, 2001, **348**, 255-262.
15. M. J. Frisch, 2016.
16. E. Cancès, B. Mennucci and J. Tomasi, *J. Chem. Phys.*, 1997, **107**, 3032-3041.
17. V. Barone, M. Cossi and J. Tomasi, *J. Chem. Phys.*, 1997, **107**, 3210-3221.
18. C. Reichardt, R. A. Vogt and C. E. Crespo-Hernández, *J. Chem. Phys.*, 2009, **131**, 224518.
19. M. Pollum, S. Jockusch and C. E. Crespo-Hernández, *J. Am. Chem. Soc.*, 2014, **136**, 17930-17933.
20. M. M. Brister and C. E. Crespo-Hernández, *J. Phys. Chem. Lett.*, 2019, **10**, 2156-2161.
21. J. J. Snellenburg, S. Laptenok, R. Seger, K. M. Mullen and I. H. M. van Stokkum, *J. Stat. Softw.*, 2012, **49**, 1-22.
22. C. E. Crespo-Hernández and B. Kohler, *J. Phys. Chem. B*, 2004, **108**, 11182-11188.
23. S. E. Krul, S. J. Hoehn, K. Feierabend and C. E. Crespo-Hernández, *J. Chem. Phys.*, 2021, **154**, 075103-075113.
24. F. Seela, C. Wei and Z. Kazimierczuk, *Helv. Chim. Acta*, 1995, **78**, 1843-1854.
25. J. Sepiol, Z. Kazimierczuk and D. Shugar, *Z. Natuforsch., b*, 1976, **31 c**, 361-370.

26. Z. Kazimierczuk, R. Mertens, W. Kawczynski and F. Seela, *Helv. Chim Acta*, 1991, **74**, 1742-1748.
27. K. Röttger, R. Siewertsen and F. Temps, *Chem. Phys. Lett.*, 2012, **536**, 140-146.
28. J. R. Platt, *J. Chem. Phys.*, 1949, **17**, 484-495.
29. J.-M. L. Pecourt, J. Peon and B. Kohler, *J. Am. Chem. Soc.*, 2000, **122**, 9348-9349.
30. J.-M. L. Pecourt, J. Peon, R. Malone, B. Kohler, N. Ismail, L. Blancafort, M. A. Robb and M. Olivucci, *J. Am. Chem. Soc*, 2001, **123**, 10370–10378.
31. P. M. Hare, C. E. Crespo-Hernández and B. Kohler, *J. Phys. Chem. B*, 2006, **110**, 18641-18650.
32. P. M. Hare, C. E. Crespo-Hernández and B. Kohler, *Proc. Natl. Acad. Sci. USA*, 2007, **104**, 435-440.
33. K. N. Rogstad, Y. H. Jang, L. C. Sowers and W. A. Goddard, *Chem. Res. Toxicol.*, 2003, **16**, 1455-1462.
34. A. Banerjee, W. Saenger, B. Lesyng, Z. Kazimierczuk and D. Shugar, *Acta Cryst.*, 1978, **34**, 2472-2477.
35. K. Dybiec and A. Gryff-Keller, *Polish J. Chem.* , 2006, **80**, 1831-1843.
36. B. Heggen, Z. Lan and W. Thiel, *Phys. Chem. Chem. Phys.*, 2012, **14**, 8137-8146.
37. B. Ashwood, L. A. Ortiz-Rodríguez and C. E. Crespo-Hernández, *J. Phys. Chem. Lett.*, 2017, **8**, 4380-4385.
38. B. Ashwood, L. A. Ortiz-Rodríguez and C. E. Crespo-Hernández, *Faraday Discuss.*, 2018, **207**, 351-374.
39. C. C.-W. Cheng, C. Ma, C. T.-L. Chan, K. Y.-F. Ho and W.-M. Kwok, *Photochem. Photobiol. Sci.*, 2013, **12**, 1351-1365.
40. F.-A. Miannay, T. Gustavsson, A. Banyasz and D. Markovitsi, *J. Phys. Chem. A*, 2010, **114**, 3256-3263.
41. J. Lee, J. R. Challa and D. W. McCamant, *J. Phys. Chem. B*, 2017, **121**, 4722-4732.
42. D. Onidas, D. Markovitsi, S. Marguet, A. Sharonov and T. Gustavsson, *J. Phys. Chem. B*, 2002, **106**, 11367-11374.
43. F. Buchner, B. Heggen, H.-H. Ritze, W. Thiel and A. Lübcke, *Phys. Chem. Chem. Phys.*, 2015, **17**, 31978-31987.